ELSEVIER

Chemical Geology 189 (2002) 55–67

CHEMICAL GEOLOGY
INCLUDING
ISOTOPE GEOSCIENCE

www.elsevier.com/locate/chemgeo

The oxidation state of iron in silicic melt at 500 MPa water pressure

Max Wilke [a,b,*], Harald Behrens [a], Dorothee J.M. Burkhard [c,d], Stéphanie Rossano [e]

[a] *Institut für Mineralogie, Universität Hannover, Welfengarten 1, D-30167 Hanover, Germany*
[b] *Institut für Geowissenschaften, Universität Potsdam, Postfach 601553, D-14415 Potsdam, Germany*
[c] *Institut für Geowissenschaften, Universität Mainz, D-55099 Mainz, Germany*
[d] *Forschangszentrum Karlsruhe, ITC-WGT, D-76021 Karlsruhe, Germany*
[e] *Wissenschaftliches Zentrum für Materialwissenschaften und Institut für Mineralogie, Universität Marburg, D-35032 Marburg, Germany*

Received 29 February 2000; accepted 22 March 2002

Abstract

The dependence of the ferric–ferrous ratio in silicate melts on oxygen fugacity was studied in the system SiO_2(Qz)–$NaAlSi_3O_8$(Ab)–$CaAl_2Si_2O_8$(An)–H_2O using Mössbauer spectroscopy. Experiments were performed under water-saturated conditions at 500 MPa, and at temperatures of 850 and 950 °C, covering a range typical for magmatic processes. The oxygen fugacity was varied in the fO_2 range from Cu–Cu_2O buffer to slightly more reducing conditions than the wüstite–magnetite buffer. The iron redox ratio was determined by analyzing the Mössbauer parameter distribution that was modeled based on experimental spectra collected at room temperature on the quenched samples. The obtained iron redox ratios show a linear dependence on oxygen fugacity on a logarithmic scale for both temperatures. The iron redox ratio (Fe^{3+}/Fe^{2+}) decreases with temperature for a given oxygen fugacity. The spectroscopic data at 850 °C are in good agreement with Fe^{3+}/Fe^{2+} ratios derived from element partitioning but show considerable deviations from iron redox ratios predicted by the empirical equation given by Kress and Carmichael [Contrib. Mineral. Petrol. 108 (1991) 82]. This indicates that an extrapolation of this equation to such low temperatures may have large errors. A sample quenched slowly through the temperature range near and below T_g shows considerable differences in the obtained Mössbauer spectra compared to more rapidly cooled samples, indicating ordering of the iron environment at least in the mesoscopic range. The oxidation state, however, does not differ when compared to the more rapidly quenched melts.

Keywords: Iron oxidation state; Silicate melt; Oxygen fugacity; Mössbauer spectroscopy

1. Introduction

The oxidation state of iron in silicate melts strongly influences the physical properties of silicate melts due to the different structural role of ferric and ferrous iron in silicate melts (e.g. Mysen, 1991). The oxidation state of iron is determined mainly by oxygen fugacity (fO_2) and temperature. In addition to these parameters, the composition of the melt may affect considerably the redox ratios of heterovalent elements (Johnston, 1964, 1965; Fudali, 1965; Sack et al., 1980; Kilinc et al., 1983; Möller and Müecke, 1984; Mysen et al., 1985; Paul, 1990; Kress and

* Corresponding author. Institut für Geowissenschaften, Universität Potsdam, Postfach 601553, 14415 Potsdam, Germany. Tel.: +49-331-977-5409; fax: +49-331-977-5060.
E-mail address: max@geo.uni-potsdam.de (M. Wilke).

0009-2541/02/$ - see front matter © 2002 Elsevier Science B.V. All rights reserved.
PII: S0009-2541(02)00042-6

Carmichael, 1991). Specifically, the addition of volatiles such as, for example, H_2O, CO_2, CH_4 to silicate melts directly influences the prevailing oxygen fugacity and, therefore, affects the redox state of the melt by internal buffering reactions, e.g.: $H_2 + 1/2\ O_2 = H_2O$ or $CO + 1/2\ O_2 = CO_2$ (e.g. Holloway and Blank, 1994). Several experimental calibrations of the Fe redox ratio to T, fO_2 and composition for volatile-free silicate melts of geological interest have been published for temperatures between 1200 and 1400 °C (Sack et al., 1980; Kilinc et al., 1983; Borisov and Shapkin, 1990; Kress and Carmichael, 1991). The effect of dissolved water in the melt on the Fe redox ratio is discussed controversially in the literature. Experiments by Moore et al. (1995) suggest that the addition of water has no influence on the Fe redox ratio in the investigated melt composition. Gaillard et al. (2001) investigated the influence of dissolved water on the redox ratio in natural silicic compositions at 200 MPa and found that measured Fe redox ratios are comparable to those predicted by the model of Kress and Carmichael (1991), which was calibrated in dry melts only. In contrast to these two studies, Baker and Rutherford (1996) found an increase of the ferric–ferrous ratio with increasing water content.

^{57}Fe Mössbauer spectroscopy may provide information on both the oxidation state and the local environment of Fe in the glass structure (e.g. Bancroft, 1973; Dyar, 1985; Spiering and Seifert, 1985; Virgo and Mysen, 1985; Mysen et al., 1985; Rossano et al., 1999). However, the broad distribution of iron environments in glasses (Alberto et al., 1996; Rossano et al., 1999) discards an assignment to discrete iron environments using two or three doublets, as done in the past (e.g. Spiering and Seifert, 1985; Virgo and Mysen, 1985; Mysen et al., 1985). In addition, one may imagine that an assignment to discrete environments might affect the estimate of the redox state, although this was shown not to be a major concern (e.g. Dunlap, 1997). In this study, we use a shape-independent distribution method (Rossano et al., 1999) that allows the direct determination of the iron redox ratio without making any assumption about the iron speciation. Iron redox ratios determined by this novel method will be compared to those derived from a conventional fit approach as proposed by Mysen et al. (1985).

To our knowledge, only one Mössbauer spectroscopic study investigated the Fe speciation in water-bearing silicic glasses (Spiering and Seifert, 1985). However, although water was present in all glasses synthesized at high pressure, none of the observed changes in the spectra is discussed in the light of the water content of the samples; all observed changes are assigned to variations in pressure of the syntheses.

In this communication, we present data on the oxidation state of Fe in hydrous silicic quenched melts determined by Mössbauer spectroscopy. The data will be used to constrain the relationship between Fe redox ratio and fO_2 at relatively low temperature (850–950 °C), a typical temperature for the formation of natural silica-rich magmas.

2. Experimental

2.1. Sample preparation

Glasses were synthesized in the haplo-tonalitic system SiO_2(Qz)–$NaAlSi_3O_8$(Ab)–$CaAl_2Si_2O_8$(An)–H_2O and were doped with 1.5 wt.% Fe_2O_3; the average composition of the dry and hydrous glass is shown in Table 1. Since the total amount of Fe in the glass is relatively low, the Mössbauer active isotope, ^{57}Fe, was enriched to 8% of ΣFe in order to enhance the signal to noise ratio of the collected Mössbauer spectra.

The anhydrous glass was synthesized from oxides and carbonates at 1600 °C with a duration of synthesis of 2 × 2 days. The glass was crushed once in between the two cycles to speed up homogenization. 200–400 mg of the resulting anhydrous glass were enclosed in $Ag_{75}Pd_{25}$ capsules together with 12 wt.% water. The glass synthesis was done in two steps. First, all capsules were annealed at 1000 °C and 500 MPa for 24 h at intrinsic oxygen fugacity to homogenize the samples in water content. After checking for mass loss by weighing, the samples were annealed in a second step under controlled oxygen fugacity. These syntheses were performed at 850 and 950 °C and 500 MPa for 24 h. The oxygen fugacity was controlled by solid buffer assemblages except for the most reducing conditions where a C–O–H sensor was applied, as described in Wilke and Behrens (1999). Experiments were usually performed in internally heated pressure

Table 1
Compositions of dry starting glass, selected syntheses and average of water-bearing glasses

	Dry glass	Hydrous 850 °C NNO	Hydrous 850 °C intrinsic	Hydrous 850 °C C–O–H	Hydrous 850 °C CCO	Hydrous 950 °C HM	Hydrous 950 °C C–O–H	Hydrous glass average
SiO_2	76.1 ± 1.9	68.42 ± 0.27	68.62 ± 0.32	68.69 ± 0.31	66.93 ± 0.52	68.64 ± 0.31	68.67 ± 0.34	68.33 ± 0.81
Al_2O_3	14.5 ± 0.9	12.93 ± 0.16	12.73 ± 0.10	12.66 ± 0.13	12.64 ± 0.17	12.75 ± 0.11	12.66 ± 0.13	12.73 ± 0.19
CaO	6.0 ± 0.6	5.09 ± 0.09	5.04 ± 0.07	5.04 ± 0.09	5.08 ± 0.11	5.07 ± 0.05	5.04 ± 0.09	5.06 ± 0.09
Na_2O	2.6 ± 0.1	1.88 ± 0.25	1.87 ± 0.41	1.88 ± 0.27	2.01 ± 0.09	2.00 ± 0.22	1.87 ± 0.3	1.92 ± 0.29
$Fe_2O_{3,tot}$	1.6 ± 0.1	1.40 ± 0.09	1.45 ± 0.07	1.43 ± 0.20	1.41 ± 0.11	1.44 ± 0.07	1.44 ± 0.22	1.42 ± 0.13
H_2O	–	10.7	10.9	10.8	11.1	10.7	11.1	10.90 ± 0.20
Total	100.8	100.42	100.61	100.50	99.17	100.70	100.78	100.36

H_2O was determined by Karl–Fischer titration, all other components by electron microprobe. Data given in wt.%.

vessels (IHPV) using Ar as pressure medium. Synthesis at Ni–NiO and Co–CoO buffer conditions were performed in cold seal pressure vessels (CSPV) with water as pressure medium. Accuracy in temperature and pressure is about ± 10 °C and ± 5 MPa for the IHPV and ± 8 °C and ± 5 MPa for the CSPV. The oxygen fugacity of runs performed under intrinsic redox conditions in the IHPV was measured by applying the NiPd redox sensor technique as described by Taylor et al. (1992) using the improved calibration by Pownceby and O'Neill (1994). Given the uncertainty in temperature, the error in the determined oxygen fugacity for the syntheses at intrinsic conditions is about ± 0.2 log units. For further details on the experimental procedure, see also Wilke and Behrens (1999). Oxygen fugacities of buffer assemblages were calculated using the data set of Robie and Hemingway (1995). The effect of pressure was included using the molar volume change at 298 K and 1 bar. After the run, the capsules were checked for a free fluid phase to ensure water-saturated conditions for all runs. Water content and compositional homogeneity of selected glasses were analyzed by Karl–Fischer titration (Behrens, 1995) and electron microprobe, respectively (Table 1).

2.2. Mössbauer spectroscopy

The Mössbauer effect was studied at the 14.4-keV emission of a ^{57}Co source embedded in Rh, using a triangular voltage, a conventional constant acceleration method and a multichannel analyzer with 1024 channels. Absorbers were carefully ground in extra dry acetone to avoid oxidation. Absorber thicknesses were optimized according to Long et al. (1983). All spectra were sampled at room temperature and calibrated against α-Fe.

Spectral analysis was done using a shape-independent distribution method (see Rossano et al., 1999 for more details). In this method, a direct determination of the Mössbauer parameter distribution is performed by fitting the experimental spectra with a large number of Lorentzian doublets having a line width of 0.25 mm/s taken from metallic iron standard (Isomer shift (IS) values vary between 0 and 2 mm/s while quadruple splitting (QS) varies in the range 0–3.5 mm/s).

The contribution of each doublet to the experimental spectrum is obtained after a quadratic minimization procedure leading to the Mössbauer parameter distribution. As ferrous iron and ferric iron do not have the same Mössbauer parameters, the ferric iron contribution to the experimental Mössbauer spectrum can be resolved and, in best cases, completely separated from the ferrous iron one. Ferric iron on total iron ratio can then be obtained by back-integrating a selected area of the parameter distribution and by calculating the ratio of the selected area to the total experimental spectrum area.

On the one hand, the uncertainty on the redox ratio determination is dependent on the signal to noise ratio of the experimental spectrum. The evaluation of this error was done by calculating the contribution to the spectrum of an area of equal surface as the one used to determine the ferric iron ratio but in an IS–QS area containing no signal. Contribution to the error from this is always lower than ± 0.02. In addition, the uncertainty on the redox ratio is affected by the fact that the Fe^{3+} doublet is hidden by the Fe^{2+} doublet, especially in Fe^{2+}-rich samples. Based on our data

analysis, we estimate the uncertainty of the resulting $Fe^{3+}/\Sigma Fe$ to be of the order of ± 0.03.

3. Results and discussion

3.1. Determination of Fe oxidation state

Mössbauer spectra of representative dry and hydrous glasses are shown in Fig. 1, and the complete set of samples synthesized together with the ferric–ferrous ratios are given in Table 2. The spectra show considerable line broadening that is typical for glasses compared to crystalline samples. Spectra are asymmetric and dominated by Fe^{2+} absorption lines. Even at highly oxidizing conditions, only a shoulder in the low velocity peak indicates the presence of Fe^{3+}.

A principal problem for the interpretation of Mössbauer spectra of glasses arises by the fact that the environment of the Fe sites is not distinct as in crystals

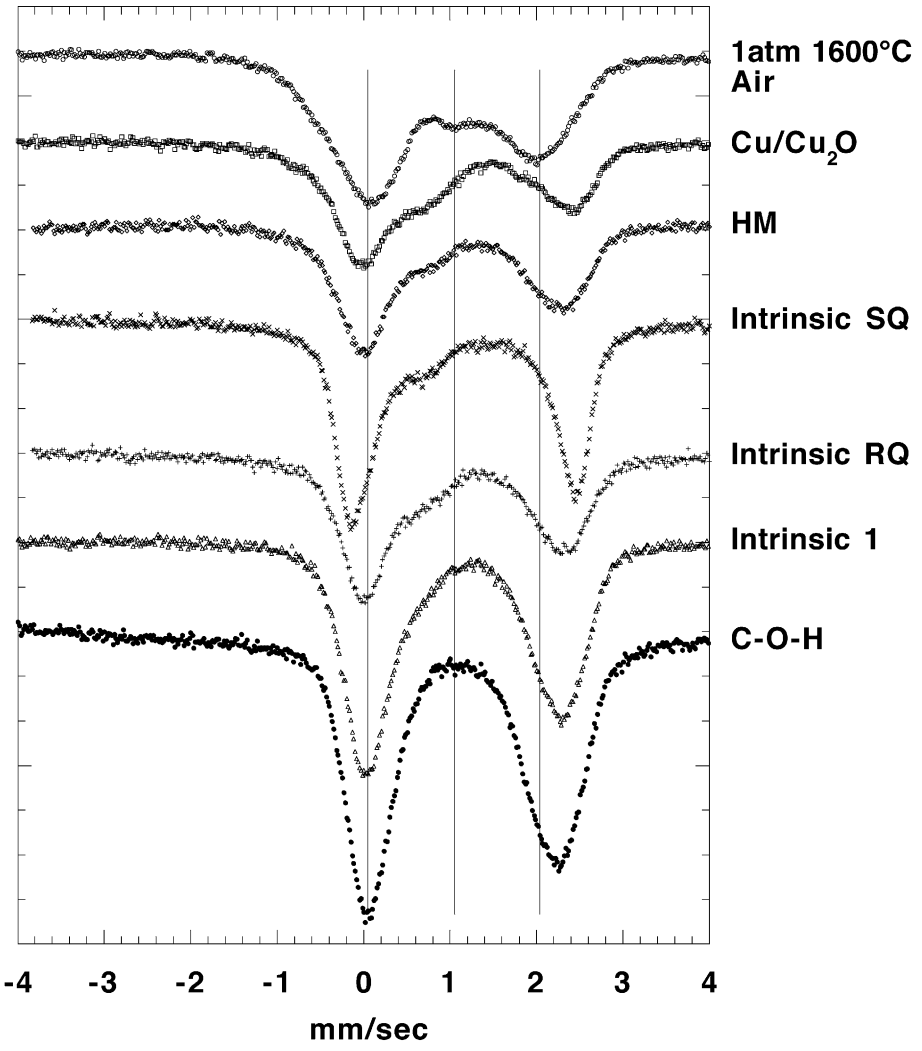

Fig. 1. Room temperature Mössbauer spectra of a set of representative samples. Spectra are calibrated against ^{57}Fe in metallic iron foil. Unless specified, spectra are taken from samples synthesized at 500 MPa and 850 °C. Cu/Cu_2O: $Cu-Cu_2O$ buffer; HM: hematite–magnetite buffer; C–O–H: C–O–H fluid sensor; SQ: slow quench; RQ: rapid quench.

Table 2
Fe redox ratios of samples determined using the shape-independent distribution analysis and conventional fitting of Lorentzian doublets

Shape-independent distribution analysis				Conventional fitting with Lorentzian doublets	
$\log f O_2$	Buffer	Fe^{3+}/Fe^{2+}	$Fe^{3+}/\Sigma Fe$	Fe^{3+}/Fe^{2+}	$Fe^{3+}/\Sigma Fe$
1 atm, 1600 C					
− 0.68	air	0.35 ± 0.05	0.26	0.56	0.36
500 MPa, 850 C					
− 15.60	C–O–H	0.03 ± 0.03	0.03	–	l.d.
− 14.04	CCO	0.03 ± 0.03	0.03	< 0.04	< 0.04
− 12.74	NNO	0.05 ± 0.03	0.05	0.04 ± 0.07	0.04
− 10.40	intrinsic	0.15 ± 0.04	0.13	0.12 ± 0.08	0.11
− 10.05	intrinsic	0.27 ± 0.05	0.21	0.25 ± 0.11	0.20
n.d.	intrinsic RQ	0.32 ± 0.05	0.24	0.30 ± 0.09	0.23
n.d.	intrinsic SQ	0.28 ± 0.05	0.22	0.32 ± 0.09	0.24
− 8.33	HM	0.3 ± 0.05	0.23	0.30 ± 0.09	0.23
− 7.60	$Cu–Cu_2O$	0.72 ± 0.09	0.42	0.75 ± 0.07	0.43
500 MPa, 950 C					
− 13.91	C–O–H	0.05 ± 0.05	0.05	–	l.d.
− 8.42	intrinsic	0.12 ± 0.04	0.11	0.11 ± 0.08	0.10
− 7.62	intrinsic	0.27 ± 0.05	0.21	0.28 ± 0.09	0.22
− 6.35	HM	0.59 ± 0.08	0.37	0.59 ± 0.09	0.37

The error on $Fe^{3+}/\Sigma Fe$ is estimated to be ± 0.03 for the shape-independent distribution analysis and ± 0.07 for the conventional fitting method. NNO: Ni–NiO; CCO: Co–CoO; HM: hematite–magnetite; C–O–H: C–O–H fluid sensor; RQ: rapid quench; SQ: slow quench.

but may vary from site to site, resulting in a distribution of the hyperfine fields. In addition, effects of hyperfine field distribution are stronger for the ferrous iron (Virgo and Mysen, 1985). Simple modeling of spectra uses Lorentzian doublets, and, frequently, one uses two doublets for ferrous iron and one for ferric iron (e.g. Virgo and Mysen, 1985; Mysen et al., 1985). One has to be aware that this choice is without structural constraint nor significance, and, conversely, the arrangement of doublets has no effect on the result of redox ratios (Helgason and Steinthosson, 1992). The inclusion of a second doublet for Fe^{2+} has, a priori, no structural significance, and the decrease in observed residuals can be taken to reflect an improved fit of the distribution of the hyperfine fields. Recent studies on tektites and synthetic Fe-bearing glass Rossano et al. (1999, 2000) found that ferrous iron is located in a continuous distribution of distorted sites between two main geometries (tetrahedron and triangular bipyramid). Hence, an improved understanding of structural features of iron-bearing glasses may be obtained from Fe Mössbauer spectra by using distributions of Lorentzian doublets (Alberto et al., 1996; Rossano et al., 1999). However, the number of distributions to take into account, again, has to be arbitrarily chosen. To avoid these drawbacks, we used a shape-independent distribution method to determine the Fe redox state (see Rossano et al., 1999 for details). This has the advantage of describing the experimental spectrum and the oxidation state of Fe without assumptions on the site occupancy and distribution.

The hyperfine parameter distribution and its projection onto the (IS,QS) plane of representative samples of dry and hydrous glasses are shown in Fig. 2. Iron redox ratios are determined from the analysis of this parameter distribution. Highly reduced glasses present only one distribution with isomer shifts ranging from 0.6 to 1.04 mm/s (Rossano et al., 1999), as it is observed for the glass synthesized at conditions of the C–O–H sensor in Fig. 2. For more oxidized glasses, a bimodal distribution of the hyperfine parameters occurs with the second distribution appearing in the low isomer shift region (Fig. 2—glass synthesized at HM buffer). This may be attributed to ferric iron as isomer shift values smaller than 0.5 mm/s are typical

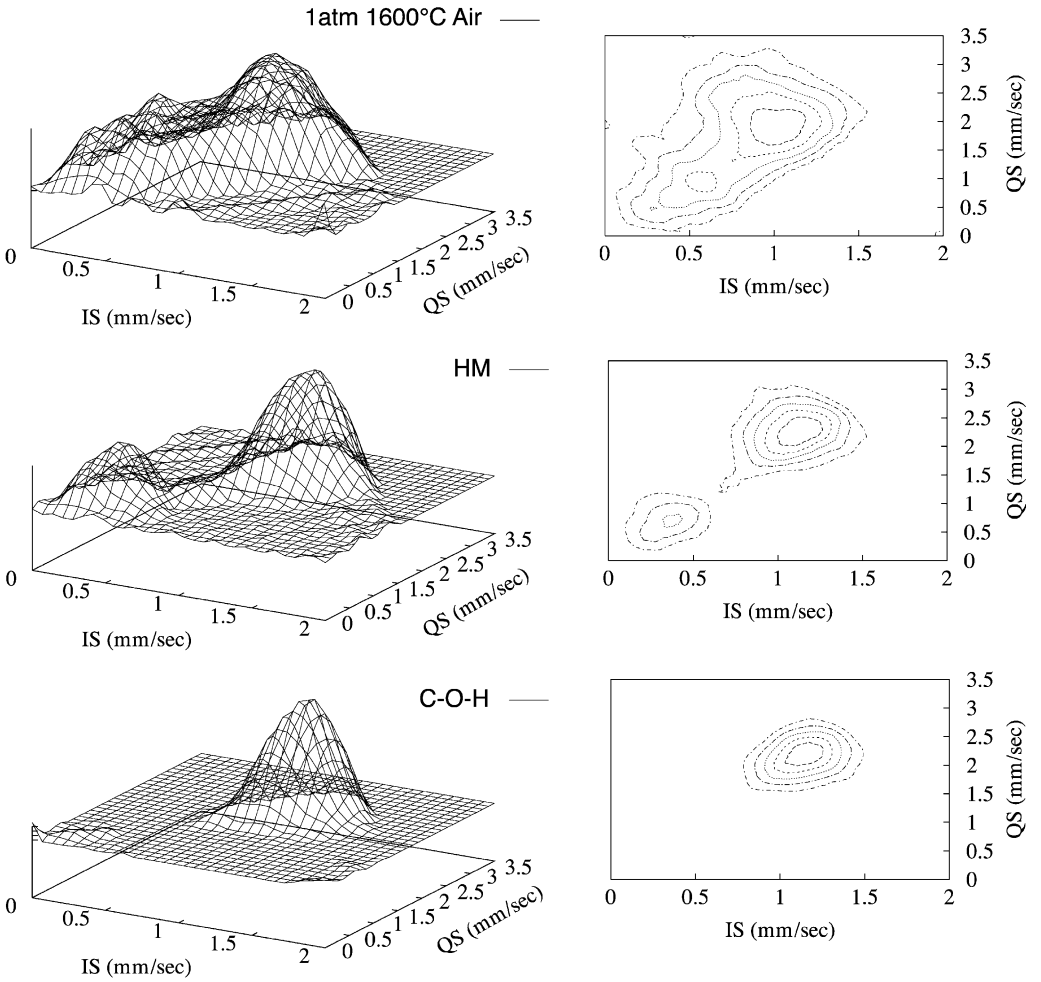

Fig. 2. Mössbauer parameter distribution and its projection onto the (IS,QS) plane for three representative samples (dry glass, hydrous oxidized and reduced glasses). Note the strong changes in the parameter distribution between dry and hydrous glass with the dry glass having a continuous overlap between the distributions of Fe^{3+} and Fe^{2+}.

for ferric iron in silicate glasses (Alberto et al., 1996). For the anhydrous glass, ferric and ferrous iron distributions overlap (Fig. 2), which makes it difficult to derive the (IS,QS) range for the ferric iron precisely. In such cases, we used isomer shift and quadruple splitting ranges derived from an oxidized but hydrous glass to evaluate the ferric iron concentration. Note that in the case of a continuous overlap of distributions, any choice of IS and QS range will be arbitrary and may affect the resulting redox ratio. The considerable difference in the observed distribution between the anhydrous and hydrous glasses may be assigned to differences in the Fe environment in these glasses (see also discussion of quench effects below). Iron redox ratios determined by the shape-independent distribution analysis for all samples are given in Table 2.

In comparison to the shape-independent distribution analysis, conventional fitting with three Lorentzian doublets, two for Fe^{2+}, and one for Fe^{3+} (as proposed by Mysen et al., 1985), provides similar redox ratios, for samples synthesized under hydrous conditions and with $Fe^{3+}/\Sigma Fe > 0.1$ (Table 2). Both methods estimate significant Fe^{3+} only if its presence is indicated by a shoulder in the spectrum. At lower

contents of Fe^{3+}, a doublet for the ferric iron may be still fitted but no clear distinction of the redox state between the samples is possible and Fe^{3+} values are within the error (samples at NNO and CCO, Table 2). The most reduced samples (synthesized at C–O–H conditions) may be described with one Fe^{2+} doublet, only. An inclusion of a doublet for Fe^{3+} does not improve the fit. The shape-independent distribution analysis, however, still shows that there is some contribution from ferric iron in these spectra (Fig. 2).

In case of the anhydrous starting glass, the two methods reveal very differing results (cf. Table 2). This difference may be attributed to the considerable overlap of the two Mössbauer parameter distributions of Fe^{2+} and Fe^{3+} in this sample (Fig. 2). Due to this overlap in distribution, the subspectra of the two Fe species cannot be separated in a proper way by either method. The doublet which is fitted for Fe^{3+} with the conventional method is shifted to higher IS compared to the hydrous samples (this shift is also seen in the experimental spectrum, see Fig. 1, 1 atm spectrum). If this shift is due to structural changes regarding Fe^{3+} only, or a result of changes in the bulk glass structure (a change which affects both Fe species) cannot be ruled out at this point. The shape-independent distribution analysis is also affected by this overlap since Fe^{3+} and Fe^{2+} signals cannot be clearly separated. As mentioned before, the (IS,QS)—area used for back-integrating the Fe^{3+}—contribution was determined from the other spectra of the oxidized hydrous samples and may underestimate the ferric iron content. Both values are significantly lower than the value that would be calculated from the equation of Kress and Carmichael (1991) ($Fe^{3+}/\Sigma Fe = 0.5$). If this equation is directly applicable to this rather simple melt composition, this would mean that both methods underestimate the Fe^{3+} content in the anhydrous sample. Wet chemical analyses performed on the anhydrous starting glass yielded $Fe^{3+}/\Sigma Fe = 0.35–0.4$, indicating that the equation may overestimate Fe^{3+} for this melt composition. These results show that the determination of Fe oxidation state from samples that show strong overlap in hyperfine parameters of Fe^{3+} and Fe^{2+} is not straight forward and results should be treated with caution.

The ferric–ferrous ratios of the hydrous samples estimated from the analysis of the Mössbauer parameter distribution are plotted versus $\log f O_2$ in Fig. 3. The values determined at 850 °C show a good linear trend on a logarithmic scale. Reliable redox ratios could be obtained at 950 °C only under oxidizing conditions. At reducing conditions ($f O_2 < f O_2$ (intrinsic)), permeation of hydrogen through the capsule wall into the IHPV is too fast and the hydrogen fugacity within the sample capsule is not buffered by the conventional buffer technique (Eugster and Wones, 1962). The determined Fe^{3+}/Fe^{2+} ratios at these reducing conditions are apparently too high for the given oxygen buffer. At very reducing conditions, a new double-capsule design made experiments possible using a C–O–H fluid to control the oxygen fugacity (Wilke and Behrens, 1999). The spectrum of the sample synthesized at such very low $f O_2$ shows no direct evidence for ferric iron in the measured spectrum but the spectral analysis indicates about 5% of Fe^{3+} which is slightly too high for the Fe redox ratio in comparison to the other samples. It is not clear whether this is due to insufficient buffering of the experiment or due to problems in the spectral analysis. However, crystallization experiments done under the same conditions did not show any evidence that the new double-capsule design did not work reliably (Wilke and Behrens, 1999). This sample highlights again the difficulty in obtaining precise redox ratios from very reduced glasses. Hence, only the syntheses performed at the hematite–magnetite buffer and at intrinsic conditions give proper constraints for the redox state of iron at 950 °C. These data show also a linear trend although it is less well constrained due to the low amount of data. Comparison with the 850 °C data suggest that for a given oxygen fugacity, the Fe redox ratio decreases with increasing temperature.

3.2. Thermodynamic modeling of the redox state of iron

The redox reaction between ferrous and ferric iron in the melt can be written as:

$$FeO + 1/4\ O_2 = FeO_{1.5} \quad (1)$$

with the equilibrium constant K_m being

$$K_m = a(FeO_{1.5})/(a(FeO) \times f O_2^{1/4}). \quad (2)$$

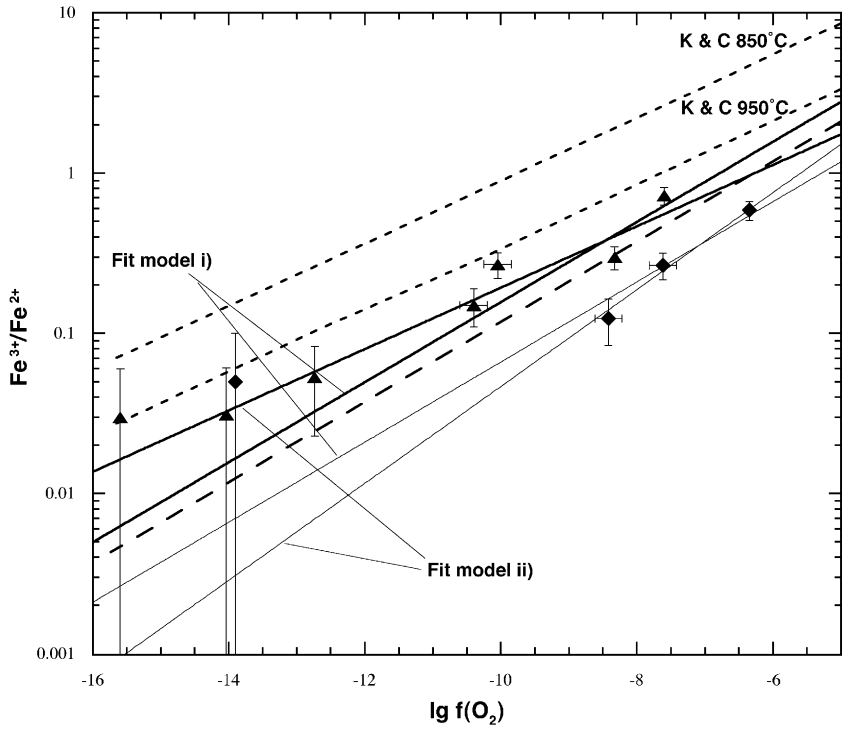

Fig. 3. Fe redox ratios determined from the Mössbauer spectra for hydrous samples. Triangles represent samples synthesized at 850 °C/500 MPa, diamonds for samples synthesized at 950 °C/500 MPa. Solid lines are fits of the data using either a constrained slope of 0.25 or an adjustable slope (see text for detail). Long-dashed line: redox ratios at 850 °C/500 MPa calculated from Fe partitioning between plagioclase and melt (Wilke and Behrens, 1999). Short-dashed line: redox ratios calculated after Kress and Carmichael (1991) for the temperatures indicated.

If we assume a constant ratio for the activity coefficients of FeO and $FeO_{1.5}$ and rearrange the equation, we may write:

$$\log(Fe^{3+}/Fe^{2+}) = 1/4 \log f O_2 + \log K_m \quad (3)$$

with (Fe^{3+}/Fe^{2+}) being the molar iron redox ratio. Therefore, if the assumption on the activity coefficients is valid, a plot of log (Fe^{3+}/Fe^{2+}) versus log fO_2 should be a straight line with a slope of 0.25.

Johnston (1964) proved this relation to be true for sodiumdisilicate glasses synthesized between 1100 and 1450 °C. However, Fudali (1965) found that for andesitic and basaltic melts at 1200 °C/1 atm, the value varies between 0.27 and 0.16 with an average value of 0.20. A deviation from ideal behavior is also reported by Mysen et al. (1985) for several melt compositions, especially for alkaline-earth alumosilicates. Regression analyses of Fe speciation data of numerous silicate melt systems yield values also close to 0.20 (Sack et al., 1980; Kilinc et al., 1983; Kress and Carmichael, 1991). The deviation from the stoichiometric value of 0.25 indicates that the assumption made on the activity coefficients is not valid, which may be attributed to nonideal mixing of components in the melt. To explain this behavior, Kress and Carmichael (1991) suggested a partial association of FeO and $FeO_{1.5}$ components in the melt.

To evaluate the dependence of the redox ratio on oxygen fugacity, we have used two fit approaches: (i) using a fixed slope of 0.25 and only K_m as an adjustable parameter, and (ii) using both slope and K_m as fit parameter. The data were weighted with the error in the determined redox ratio as given by the error bars in Fig. 3. At 850 °C, the fit model (ii) converged to a slope lower to that expected from the stoichiometric

reaction (0.19 ± 0.03 instead of 0.25). This value of the slope comes close to the value given by Kress and Carmichael (1991). However, when the error of both fit parameters is considered, the deviation from 0.25 is still within the uncertainty of the data (Table 3). We consider that the data are sufficiently well described using the ideal value (0.25). The fitted K_m values are 50 ± 4 and 16 ± 9 for fit models (i) and ii), respectively. The large uncertainty of K_m from fit (ii) indicates that the amount and quality of data are insufficient for a two-parameter fit.

The discrepancy between the two fit models is considerably larger for the 950 °C data, yielding a slope 0.30 ± 0.06 for the fit model (ii). However, the fO_2 range and the amount of data are too small for an accurate two-parameter fit in this case.

For comparison, iron redox ratios calculated with the empirical equation of Kress and Carmichael (1991) are included in Fig. 3. This equation is based on previous calibrations from Sack et al. (1980) and Kilinc et al. (1983) using a large data set of chemical analyses of dry glasses equilibrated at temperatures between 1200 and 1400 °C under controlled redox conditions. The effect of pressure was added by Kress and Carmichael (1991) using compressibility data of Fe-bearing melts.

Redox ratios calculated with this equation are considerably higher than the measured values (by up to one order of magnitude at reducing conditions). Redox ratios calculated after Kilinc et al. (1983) for this melt composition are similar to that after Kress and Carmichael (1991) due to the small change in molar volume in the redox reaction (Eq. (1)). Observed deviations between the calculated and measured redox ratios may be explained either by the high water content of the samples in this study or by the large difference in the temperature of the syntheses to those of the data set used for the equation. An effect of water on the Fe redox state cannot be totally excluded by our study since water content and temperature were not varied independently. However, since Moore et al. (1995) found virtually no effect of water on the ferric–ferrous ratio in water-saturated melts between 100 and 500 MPa at constant temperature, we conclude that the observed deviations may be mainly due to temperature effects.

Table 3
Fit parameters obtained for Eq. (3) using the two fit models and the data sets shown

	850 °C, Fit model (i)	850 °C, Fit model (ii)	950 °C, Fit model (i)	950 °C, Fit model (ii)
K_m	50 (4)	16 (9)	21 (2)	49 (45)
Slope	0.25 (fixed)	0.19 (0.03)	0.25 (fixed)	0.30 (0.06)
R^2	0.850	0.880	0.944	0.971
No. samples used for fit	7	7	4	4

The controversy between the studies of Moore et al. (1995) and, to some extent, Gaillard et al. (2001) to the one of Baker and Rutherford (1996) on the effect of water on the Fe redox state, however, may be explained with the different experimental approach used in the studies. In contrast to Moore et al. (1995), Baker and Rutherford varied the water content of the system at constant pressure and constant buffer conditions using the double-capsule technique. The oxygen fugacity is controlled via the equilibrium in hydrogen fugacity across the capsule wall between buffer assemblage and sample. Oxygen fugacities in sample and buffer assemblage are only equal if both are at water-saturated conditions. Any variation in the water activity in the sample will affect the prevailing oxygen fugacity since the hydrogen fugacity is fixed externally by the buffer assemblage. Thus, the variation of the redox ratio with water content observed by Baker and Rutherford (1996) may simply be caused by a variation in the oxygen fugacity and gives no information on the effect of the dissolved water on the Fe species present in the melt. Gaillard et al. (2001) studied the effect of water only for water-saturated conditions at a single pressure (200 MPa) by comparing their experimental results to the equation of Kress and Carmichael (1991). In contrast to our results, Gaillard et al. (2001) found only minor deviations from that equation. The reason for these differing observations is not clear but may reflect the fact that those authors performed syntheses at higher temperatures (930–1000 °C) and lower pressure.

The discrepancy in the relationship to fO_2 (slope) of our data to the relationship given by the empirical equations of Kress and Carmichael (1991) and previous studies of Sack et al. (1980) and Kilinc et al. (1983) may be attributed to the data set used to

calibrate these models. Most of the samples were equilibrated at oxidizing conditions. Further, ferric–ferrous ratios were obtained mainly by combining wet chemical measurements of ferrous iron with determination of total iron. This method has therefore a relatively large error if used on reduced samples since only the ferrous iron is measured directly and ferric iron is derived by difference to total iron. Finally, oxidation of a small part of Fe^{2+} during preparation for the analysis can produce a systematic error, which increases with decreasing Fe^{3+}/Fe^{2+}. As pointed out by Fudali et al. (1987) and Fudali (1988), a direct determination of the ferric species seems to be necessary at low fO_2. The fact that the results of Gaillard et al. (2001) are rather consistent with the equation of Kress and Carmichael (1991) (see also above) may indicate as well an influence of the method used for the determination of the oxidation state. Gaillard et al. (2001) used a method similar to the one used for the calibration the equation of Kress and Carmichael (1991).

In contrast to the empirical equations, the redox ratios determined by Mössbauer analysis are in good agreement with iron redox ratios extracted from Fe-partitioning data between plagioclase and a melt similar in composition as used in this study (Wilke and Behrens, 1999) as shown in Fig. 3. In that study, K_m was determined by modeling of the fO_2 dependence of the experimental partition coefficients assuming an ideal stoichiometry of the redox equilibrium in the melt. Thus, both direct and indirect determinations of the Fe redox ratio in these melt systems are consistent with ideal mixing behavior in the melt, i.e. the ratio of the activity coefficients of FeO and $FeO_{1.5}$ does not change significantly in the investigated redox range. However, it has to be emphasized that the iron oxide content is relatively low in our melts (ca. 1.5 wt.%), therefore both FeO and $FeO_{1.5}$ components are expected to be in the Henry's law region. Deviations from Henry's law may occur at higher contents.

3.3. Effect of quench rate

A few experiments were performed to investigate the effect of the quench rate on Fe oxidation state in the glasses. In addition to experiments using the normal quench rate (decreasing from ca. 150 K/min above 500 °C to 100 K/min below 500 °C), runs were performed with faster or lower quench rate. For the rapid quench run (RQ), we have used a device in the IHPV which allows dropping of the sample from the hot spot of the furnace to the cold part of the vessel. The quench rate for this device is estimated to be >150 K/s. The slow quench run (SQ) was performed by quenching the sample with the normal rate to 360 °C (just above the temperature of glass transition, T_g), followed by slow cooling with a rate of 1 K/min through T_g down to room temperature. The temperature of T_g was estimated to be 250–350 °C for hydrous tonalitic melts, based on viscosity data (Schulze, 2000).

Observations made by polarization microscopy and X-ray diffraction have shown no evidence for crystallites in any of the experiments. No differences could be observed in the Mössbauer spectrum collected from the rapidly quenched sample in comparison to the normally quenched samples (Fig. 1, RQ). This indicates that the quench rates normally achieved in these IHPV yield similar results as provided by higher quench rates. In contrast, the slowly quenched sample shows significant differences in the Mössbauer spectrum compared to the rapidly quenched sample (Fig. 1, SQ). The width of the observed asymmetric doublet is considerably smaller indicating a narrower distribution, and hence, the beginning of an ordering/crystallization process (Fig. 1, SQ). In addition, the maximum of the probability distribution is at higher IS and QS (Fig. 4, SQ). This may be attributed to a change in iron speciation. Although the observed spectrum of the sample changed considerably, the determined redox ratio in the sample did not change significantly compared to the rapidly quenched glass. This result is in agreement with observations of Dyar et al. (1987), who found virtually no effect of the quench rate on the redox ratio of quenched melts. The dependence of the spectra on the quench rate of the sample indicate that even at those low temperatures close to T_g, local ordering processes take place and that the environment of Fe in the glass structure is sensitive to the thermal history of the sample around T_g. The resulting "ordered units" in the glass are only very small in size (probably below 100 Å, see also Farges et al., 2001) so that they are not detectable as crystals by standard methods like XRD or polarization microscopy.

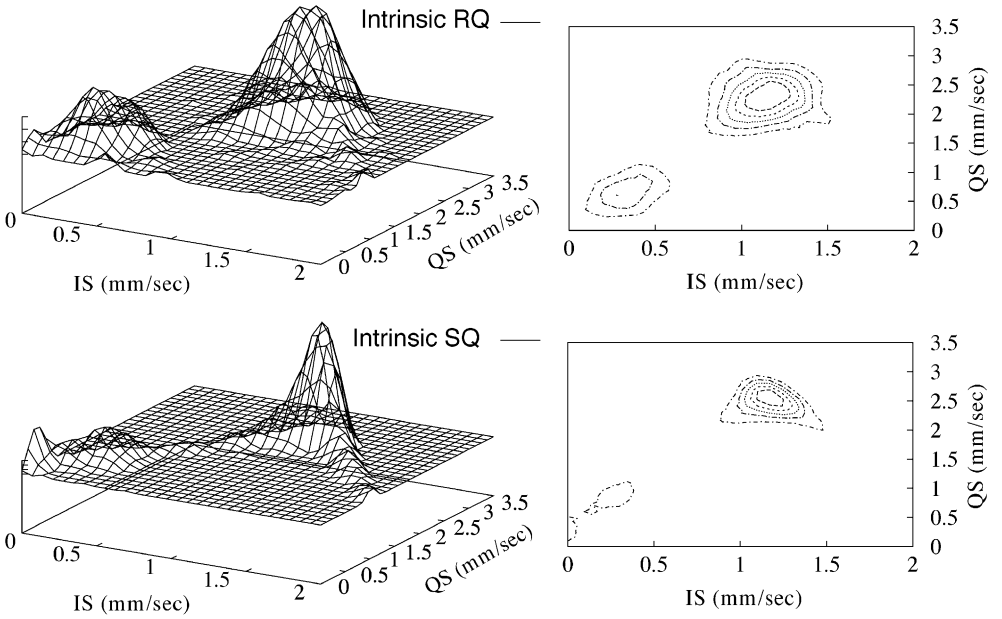

Fig. 4. Mössbauer parameter distribution and its projection onto the (IS,QS) plane for the slowly (SQ) and rapidly quenched (RQ) sample, respectively.

In the light of these observations, we would like to note that the differences observed in the distribution of hyperfine fields between the anhydrous and hydrous glasses, which indicate a significant change in the structural environment of Fe, may not necessarily be explained by dissolution of water in these melts. Instead, the clearly bimodal distribution found in the hydrous glasses may just be a product of the quench process which, even at the highest quench rate, is insufficient to freeze in the species present in the melt. Ordered domains in glasses containing transition metals were also detected by other authors. A combination of TEM, Raman and EXAFS study of Ni in hydrous albitic glasses suggested the presence of nanocrystalline phyllosilicate domains (30–50 Å in average diameter) in these glasses (Farges, et al. 2001). A complete evaluation of the coordination chemistry of Fe in these glasses, however, is beyond the scope of this paper and will be discussed elsewhere.

It is interesting to note that a strong effect of iron on properties of silicate melts around the glass transition was also observed in other studies. For instance, in viscosity measurements on supercooled melts with natural Fe-bearing melt composition, an increase of the viscosity with experimental duration was observed (Richet et al., 1996). The oxidation state of Fe did not change during those experiments and the authors attribute the change in viscosity to a change of the melt composition by partial crystallization induced by the presence of Fe, in agreement with recent observations (Burkhard, 2001). Ordering is certainly the precursor for the formation of substructural units and final crystallization. Such substructural units were suggested to determine physical bulk properties of supercooled magmatic systems (Burkhard, 2000).

4. Summary and conclusions

Fe^{2+}/Fe^{3+} ratios in hydrous tonalitic melts derived from Mössbauer spectra are relatively insensitive to the method used for extracting the species concentration from the spectra. The shape-independent distribution analysis of the hyperfine parameters, however, has advantages for samples with $Fe^{3+}/\Sigma Fe < 0.1$. The main advantage of the shape-independent distribution analysis is that it provides a quantitative estimate of the site distribution of Fe and visualizes overlaps in the parameter distribution of Fe^{3+} and Fe^{2+}. Overlapping

Mössbauer parameter distributions for Fe^{3+} and Fe^{2+} may affect the determination of the Fe oxidation state. The resulting Fe^{3+}/Fe^{2+} ratios are much lower than predictions by the model of Kress and Carmichael (1991). The discrepancy may be mainly related to insufficient calibration of the model at low temperature as dissolved water probably has only minor effects in accordance to results by Moore et al. (1995). Our study shows that the application of the equations by Kress and Carmichael (1991), Kilinc et al. (1983) and Sack et al. (1980) at such low temperatures must be treated with caution.

Acknowledgements

Technical assistance during the sample synthesis by W. Hurkuck and B. Aichinger and sample preparation by O. Diedrich are highly appreciated. We thank J. Klein, formerly at the Universität Marburg, for help in spectrum acquisition. We would like to thank F. Farges for enthusiastic and fruitful discussions. Helpful comments by M.D. Dyar and H.S.C O'Neill are gratefully acknowledged. This study was funded by the Deutsche Forschungsgemeinschaft, Schwerpunktprogramm Elementverteilung (Project Be/1720/4). **[RR]**

References

Alberto, H.V., Pinto da Cunha, J.L., Mysen, B.O., Gil, J.M., Ayres de Campos, N., 1996. Analysis of Mössbauer spectra of silicate glasses using a two-dimensional Gaussian distribution of hyperfine parameters. J. Non-Cryst. Solids 194, 48–57.

Baker, L.L., Rutherford, M.J., 1996. The effect of dissolved water on the oxidation state of silicic melts. Geochim. Cosmochim. Acta 60, 2179–2187.

Bancroft, G.M., 1973. Mössbauer spectroscopy. Introduction for Inorganic Chemists and Geochemists. Wiley, New York.

Behrens, H., 1995. Determination of water solubilities in high-viscosity melts: an experimental study on $NaAlSi_3O_8$ and $KAlSi_3O_8$ melts. Eur. J. Mineral. 7, 905–920.

Borisov, A.A., Shapkin, A.I., 1990. A new empirical equation rating Fe^{3+}/Fe^{2+} in magmas to their composition, oxygen fugacity, and temperature. Geochem. Int. 27, 111–116.

Burkhard, D.J.M., 2000. Iron-bearing silicate glasses at ambient conditions. J. Non-Cryst. Solids 275, 175–188.

Burkhard, D.J.M., 2001. Crystallization and oxidation of Kilauea basalt glass: processes during reheating experiments. J. Petrol. 42, 507–527.

Dunlap, R.A., 1997. An investigation of Fe oxidation states and site distributions in a Tibetan tektite. Hyperfine Interact. 110, 217–225.

Dyar, M.D., 1985. A review of Mössbauer data on inorganic glasses: the effects of composition on iron valency and coordination. Am. Mineral. 70, 304–316.

Dyar, M.D., Naney, M.T, Swanson, S.E., 1987. Effects of quench methods on Fe^{3+}/Fe^{2+} ratios: a Mössbauer and wet chemical study. Am. Mineral. 72, 792–800.

Eugster, H.P., Wones, D.R., 1962. Stability relations of the ferruginous biotite, annite. J. Petrol. 3 (Part 1), 82–125.

Farges, F., Munoz, M., Siewert, R., Malavergne, V., Brown Jr., G.E., Behrens, H., Nowak, M., Petit, P.-E., 2001. Transition elements in water-bearing silicate glasses/melts: Part II. Ni in water-bearing glasses. Geochim. Cosmochim. Acta 65, 1679–1693.

Fudali, R.F., 1965. Oxygen fugacities of basaltic and andesitic magmas. Geochim. Cosmochim. Acta 29, 1063–1075.

Fudali, R.F., 1988. Effects of quench methods on Fe^{3+}/Fe^{2+} ratios: discussion. Am. Mineral. 73, 1478.

Fudali, R.F., Dyar, M.D, Griscom, D.L., Schreiber, H.D., 1987. The oxidation state of iron in tektite glass. Geochim. Cosmochim. Acta 51, 2749–2756.

Gaillard, F., Scaillet, B., Pichavant, M., Beny, J.M., 2001. The effect of water and fO_2 on the ferric–ferrous ratio of silicic melts. Chem. Geol. 174, 255–273.

Helgason, Ö., Steinthosson, S., 1992. Rates of redox reactions in basaltic melts determined by Mössbauer spectroscopy. Hyperfine Interact. 70, 985–988.

Holloway, J.R., Blank, J.G., 1994. Application of experimental results to C–O–H species in natural melts. Rev. Miner. 30, 187–230.

Johnston, W.D., 1964. Oxidation–reduction equilibria in iron-containing glass. J. Am. Ceram. Soc. 47, 198–201.

Johnston, W.D., 1965. Oxidation–reduction equilibria in molten $Na_2O–SiO_2$ glass. J. Am. Ceram. Soc. 48, 184–190.

Kilinc, A., Carmichael, I.S.E., Rivers, M.L., Sack, R.O., 1983. The ferric–ferrous ratio of natural silicate liquids equilibrated in air. Contrib. Mineral. Petrol. 83, 136–140.

Kress, V.C., Carmichael, I.S.E., 1991. The compressibility of silicate liquids containing Fe_2O_3 and the effect of composition, temperature, oxygen fugacity and pressure on their redox states. Contrib. Mineral. Petrol. 108, 82–92.

Long, G.T., Cranshaw, T.E., Longworth, G., 1983. The ideal Mössbauer effect absorber thickness. Mossbauer Eff. Ref. Data J. 6, 42–49.

Möller, P., Muecke, G.K., 1984. Significance of Europium anomalies in silicate melts and crystal-melt equilibria: a reevaluation. Contrib. Mineral. Petrol. 87, 242–250.

Moore, G., Righter, K., Carmichael, I.S.E., 1995. The effect of dissolved water on the oxidation state of iron in natural silicate liquids. Contrib. Mineral. Petrol. 120, 170–179.

Mysen, B.O., 1991. Relations between structure, redox equilibria of iron, and properties of magmatic liquids. In: Perchuk, L.L., Kushiro, I. (Eds.), Advances in Physical Chemistry, vol. 9, pp. 41–98.

Mysen, B.O., Virgo, D., Neumann, E.R., Seiffert, F.A., 1985. Redox equilibria and the structural states of ferric and ferrous iron in melts in the system $CaO–MgO–Al_2O3–SiO_2–Fe–O$: relation-

ships between redox equilibria, melt structure and liquidus phase equilibria. Am. Mineral. 70, 317–331.

Paul, A., 1990. Oxidation–reduction equilibrium in glass. J. Non-Cryst. Solids 123, 354–362.

Pownceby, M.I., O'Neill, H.S.C., 1994. Thermodynamic data from redox reactions at high temperatures: III. Activity–composition relations in Ni–Pd alloys from EMF measurements at 850–1250 K, and calibration of the NiO+Ni–Pd assemblage as a redox sensor. Contrib. Mineral. Petrol. 116, 327–339.

Richet, P., Lejeune, A.M., Holtz, F., Roux, J., 1996. Water and the viscosity of andesite melts. Chem. Geol. 128, 185–197.

Robie, R.A., Hemingway, B.S., 1995. Thermodynamic properties of minerals and related substances at 298.15 K and 1 bar (10^5 Pascals) pressure and at higher temperatures. U.S. Geol. Surv. Bull. 2131, 461 pp.

Rossano, S., Balan, E., Morin, G., Bauer, J.-Ph., Calas, G., Brouder, Ch., 1999. ^{57}Fe Mössbauer spectroscopy of tektites. Phys. Chem. Miner. 26, 530–538.

Rossano, S., Ramos, A., Delaye, J.-M., Creux, S., Filipponi, A., Brouder, C.H., Calas, G., 2000. EXAFS and molecular dynamics combined study of CaO–FeO–$2SiO_2$ glass. New insights into site significance in silicate glasses. Euphys. Lett. 49, 597–602.

Sack, R.O., Carmichael, I.S.E., Rivers, M., Ghiorso, M.S., 1980. Ferric–ferrous equilibria in natural silicate liquids at 1 bar. Contrib. Mineral. Petrol. 75, 369–376.

Schulze, F., 2000. Untersuchung zum Einfluss von Druck und geloestem Wasser auf die Viskositaet silikatischer Schmelzen: Anwendung eines ''parallel-plate''—Viskosimeters unter hohen Druecken. PhD Thesis, University of Hannover, Germany.

Spiering, B., Seifert, F.A., 1985. Iron in silicate glasses of granitic composition: a Mössbauer spectroscopic study. Contrib. Mineral. Petrol. 90, 63–73.

Taylor, J.R., Wall, V.J., Pownceby, M.I., 1992. The calibration and application of accurate redox sensors. Am. Mineral. 77, 284–295.

Virgo, D., Mysen, B.O., 1985. The structural state of iron in oxidized vs. reduced glasses at 1 atm: a ^{57}Fe Mössbauer study. Phys. Chem. Miner. 12, 65–76.

Wilke, M., Behrens, H., 1999. The dependence of the partitioning of iron and europium between plagioclase and hydrous tonalitic melt on oxygen fugacity. Contrib. Mineral. Petrol. 137, 102–114.